miR-148a inhibits self-renewal of thyroid cancer stem cells via repressing INO80 expression

WEIZHONG SHENG*, YUSHENG CHEN*, YUDA GONG, TIANGENG DONG, BO ZHANG and WEIDONG GAO

Department of General Surgery, Zhongshan Hospital, Fudan University, Shanghai, P.R. China

Received February 5, 2016; Accepted August 23, 2016

DOI: 10.3892/or.2016.5203

Abstract. Anaplastic thyroid carcinoma (ATC) is aggressive and lethal with extrathyroidal invasion, distant metastasis, and resistance to conventional therapies. Cancer stem cells (CSCs) are proposed to be responsible for high recurrence rate in ATC. MicroRNAs (miRNAs) have recently been found as an important class of cellular regulators of ATC carcinogenesis. Identification of CSC-related miRNAs and targets is therefore a priority for the development of new therapeutic paradigms. Patient-derived ATC cells were cultured in conditional media on poly-hema-treated dish. ATC CSCs were isolated and enriched through as a series of steps including initial isolation of sphere-forming CSC population, subsequent amplification of this CSC population in a xenograft model treated with cisplatin, and purification of CSCs from xenograft tumors followed by final enrichment using sphere-forming assays. Expression of CSC markers was measured by flow cytometry, immunofluorescence staining, qPCR and western blot analyses. Expression of miRNAs in ATC-CSCs was profiled by microarray analysis. Proliferation and differentiation rates were determined based on the size of spheres formed *in vitro* and tumors formed *in vivo*. We successfully isolated and enriched an ATC-CSC population. We identified 17 miRNAs differentially expressed in primary ATC cells vs. ATC-CSCs, among which miRNA-148a was significantly downregulated in ATC-CSCs. Overexpression of miRNA148a in ATC-CSCs induced cell cycle arrest and loss of stem cell characteristics. In addition, we identified INO80 as a target gene of miR-148a. The expression of INO80 was upregulated in ATC-CSCs and downregulated upon miRNA-148 overexpression. Overexpression of miRNA-148a and knockdown of INO80 acted synergistically to decrease the expression of stem cell marker genes as well as to attenuate stem cell-specific properties including the ability to form tumors. This study identified novel contrasting roles for miR-148a and INO80 in the regulation of the stemness of ATC-CSCs and their capacity to initiate tumor formation. Our findings may open a new avenue for therapeutic development against ATC that targets INO80 in the CSCs through enhancing miRNA-148a levels.

Correspondence to: Dr Weidong Gao, or Dr Bo Zhang, Department of General Surgery, Zhongshan Hospital, Fudan University, 180 Feng Lin Road, Shanghai, P.R. China
E-mail: gao.weidong@zs-hospital.sh.cn
E-mail: zhang.bo@zs-hospital.sh.cn

*Contributed equally

Key words: anaplastic thyroid carcinoma, cancer stem cells, miR-148a, INO80

Introduction

Thyroid cancer has increased rapidly in recent decades. Anaplastic thyroid carcinoma (ATC) is the most aggressive type in thyroid malignancies with extra thyroidal invasion, distant metastasis, and resistance to conventional therapies. Accordingly, 90% of patients with ATC die within 6 months of diagnosis, accounting up to 14-39% of all thyroid cancer-related deaths annually (1). ATC is derived from pre-existing or coexisting papillary or follicular thyroid cancer cells through the sequential accumulation of genetic mutations during the proliferation of mature thyroid follicular cells (2). In many cases, patients with ATCs also harbor a pre-existing or coexisting well-differentiated thyroid cancer of follicular origin. These events are accompanied by a dedifferentiation process that occurs as the cancer cells acquire the neoplastic phenotype, with a marked epithelial to mesenchymal transition (3).

Attempts to identify biological markers that would facilitate targeted therapy have led to the realization that thyroid cancer might originate from cancer stem cells (CSCs). Though self-renewal and differentiation capacity are hallmark traits of normal stem cells, CSCs are found to also possess the high proliferative capacity and phenotypic plasticity (4). These similarities have given rise to the hypothesis that the CSCs are a subpopulation of cancer cells possessing tumor-initiating capability (5-7). In light of several pivotal studies, the existence of 'stem-like' cells or CSCs has been demonstrated in various types of solid cancer including ATC (8-15). Further studies have shown that CSCs possess typical characteristics of normal thyroid stem cells and are thought to give rise to all ATC cells.

Existing evidence suggests that the present treatments of ATC may not be effective at targeting ATC-CSCs (15,16). Whether CSCs simply are tumor cells at undifferentiated stage remains undetermined, one key molecular characteristic of

CSCs is their capability of extensive proliferation and spherical clone formation in suspension culture conditions (17). To better understand the mechanisms underlying the involvement of CSCs in ATC, vigorous effort has been devoted to the isolation of putative CSCs. Tumor sphere-forming assays have been widely applied to identify potential CSC populations (18). CSCs can also be isolated using flow cytometry according to the expression of specific cell surface markers, such as CD133 and CD44 (19,20). Both methods, however, are technically challenging, laborious and time-consuming with varying degrees of success. In this regard, this study has established a new experimental strategy to reliably isolate and enrich CSC population in ATC cells.

MicroRNAs (miRNAs) are a class of endogenous noncoding small RNAs playing important roles in tumor formation (21-23). Recent evidence suggests that many miRNAs are functionally linked to the carcinogenesis of ATC due to their roles in regulating the target genes involved in different cell signaling pathways (24-26). By using the isolated CSCs as a model, we screened the miRNA expression profiles and identified miRNA-148a and its target INO80 as important regulators of the stem cells characteristics of ATC-CSCs. Furthermore, our functional analysis provided evidence demonstrating that the inversed expression of microRNA-148a and INO80 is critical for CSCs to maintain their proliferative and tumor-forming capacity.

Materials and methods

Cell culture. The tumor tissues were obtained from 15 female patients (pathological and clinical features are shown in Table I) with biopsy-diagnosed anaplastic thyroid carcinoma. These patients had received chemotherapy followed by modified radical thyroidectomy. Written informed consent was obtained from each individual, which was approved by the Biomedical Research Ethics Committee of Affiliated Zhongshan Hospital of Fudan University (no. 201102). All samples were received in the laboratory within 20 min of surgery and immediately mechanically disaggregated, then digested with 0.25% trypsin-EDTA for 15 min. Disaggregated tumor cells were cultured in RPMI-1640 supplemented with 10% fetal bovine serum (FBS; Gibco, Grand Island, NY, USA), 2 mM glutamine, 100 U/ml penicillin, and 100 μg/ml streptomycin (all from Cambrex, Walkersville, MD, USA). At 80% confluence, cells were treated with 40 μmol/l cisplatin (Sigma) and 10 μmol/l paclitaxel (Sigma) for 24 h. Drug-resistant cells were maintained and subcultured with 0.25% trypsin-EDTA for 1-2 min at 37˚C. The selected cancer cells were then cultured under stem cell conditions by resuspension in serum-free DMEM/F12 supplemented with 5 μg/ml insulin (Sigma-Aldrich, St. Louis, MO, USA), 10 ng/ml human recombinant epidermal growth factor, 10 ng/ml basic fibroblast growth factor (both from Invitrogen, WA, USA), 12 ng/ml leukemia inhibitory factor (Gibco), and 10 ng/ml noggin. Cells grown under these conditions formed non-adherent mammospheres after enzymatically dissociated with 0.25% trypsin-EDTA for 1-2 min at 37˚C every three days.

Animals. NOD-SCID nude mice, 4 weeks of age, were purchased from Shanghai Laboratory Animal Co. Mice were kept under pathogen-free conditions according to the standard guidelines of the Institutional Animal Care and Use Committee.

Chemoresistant tumor model. Chemoresistant tumor models established in this study were approved by the Biomedical Research Ethics Committee of Affiliated Zhongshan Hospital of Fudan University (no. 201113). Subcutaneous xenografts were established with mammospheres obtained as above. Indicated dissociated cell numbers from mammospheres were injected subcutaneously into the mammary fat pads of female BALB/c-nu/nu mice. Cisplatin treatments started once the size of the xenograft reached 5 mm in diameter. Mice were randomly assigned to four groups (each n=3), treated with cisplatin intraperitoneally at 0, 1, 2 or 4 mg/kg every 4 days for 4 weeks. The tumor volume was calculated as follows, tumor volume (mm^3) = L x W^2 x 0.4. Mice were sacrificed by cervical dislocation. Tumor xenografts were harvested, weighed and underwent immunohistochemical (IHC) analysis. The presence of tumors was confirmed by necropsy.

Lentiviral vector production. Oligonucleotides encoding miR148a pre-miRNA was synthesized according to previously published sequences and cloned in the lentiviral vector (lenti-mir). ShRNA target INO80 were cloned into PLKO.1 lentiviral vector. Lentiviral vectors were produced by transient transfection of 293T cells. Briefly, the transfection mixture consisted of 20 μg lentiviral vectors, 10 μg pSPAX and 5 μg pMD2.G (kindly provided by Didier Trono). The volume of mixture was adjusted to 250 μl with H_2O. Then 250 μl of 0.5 M $CaCl_2$ was added to the solution. Subsequently 500 μl of 2X HeBS (0.28 M NaCl, 0.05 M HEPES, 1.5 M Na_2HPO_4) was added. The final solution was left to incubate for 30 min. The culture dishes were placed into a 37˚C humidified incubator with 5% CO_2. Fourteen hours later the medium was aspirated and 10 ml of fresh DMEM-10% FBS, prewarmed to 37˚C, was gently added. Cultures were further incubated for 28 h, after which virus was collected. Concentrated supernatants were titrated with serial dilutions of vector stocks on $1x10^5$ HeLa cells followed by fluorescence-activated cytometric analysis (Beckton-Dickinson Immunocytometry Systems). Titer of lenti-EGFP vectors were calculated to be between 0.1-$1x10^9$ TU/ml according to the formula: $1x10^5$ HeLa cell x % EGFP-positive cell x 1,000/μl virus (data not shown).

Quantitative reverse transcription PCR and mRNA expression analyses. Total RNA from samples was harvested using TRIzol (Invitrogen) and miRNeasy mini kit (Qiagen) according to the manufacturer's instructions. RNA quantity was measured using the NanoDrop 1000. The samples were then labeled using the miRCURY™ Hy3™/Hy5™ Power labeling kit and hybridized on the miRCURY™ LNA Array (v.18.0). Replicated miRNAs were averaged and miRNAs with intensities ≥30 in all samples were chosen for calculating the normalization factor. Expressed data were normalized using the median normalization.

Total RNA was extracted from cells using TRIzol reagent (Invitrogen) and treated with DNase I (Promega), according to the manufacturer's instructions. Then the cDNA was synthesized using SuperScript II reverse transcriptase (Invitrogen).

Table I. Baseline characteristics for all patients (n=15).

Characteristics	No. of patients
Age, years	
<65	10
≥65	5
Gender	
Female	15
Charlson-Deyo comorbidity score	
0	10
1	4
≥2	1
Tumor size	
<6	7
≥6	8
Metastasis	
Yes	6
No	9
WBC count	
$<1x10^{10}$	9
$\geq 1x10^{10}$	6
Chemotherapy	
Yes	15
Surgical margins	
Negative	11
Positive	4
Surgery	
Radical thyroidectomy	15

For quantitative gene expression analyses, cDNA was subjected to PCR amplification using Sybr Green I (Invitrogen) and the ABI PRISM 7700 system (Applied Biosystems, Foster City, CA, USA) for real-time detection of PCR products. The housekeeping gene 18S RNA served as the internal reference and was amplified parallel to the gene of interest for every template, in a separate reaction tube. Mean mRNA ratios, representing gene expression relative to the b-Gus reference gene, were calculated as the means of five individual mRNA ratios assessed in five independently performed PCR reactions. The primer sequences of all genes for PCR are as follows: 18S, 5'-CGTTGATTAAGTCCCTGCCCTT-3'; 5'-TCAAGTTCGACCGTCTTCTCA-3'. CD133, 5'-TGGATGCAGAACTTGACAA-3'; 5'-ATACCTGCTACGACAGTCGTG-3'. SOX-2, 5'-CCTGGCAGCTGGAAGACAAAT-3'; 5'-TCCTCCAAATGCAATCACAG-3'. OCT-4, 5'-GGCCCGAAAGAGAAAGCG-3'; 5'-ACCCAGCAGCCTCAAAATCCTC-3'. Nanog, 5'-GGGCCTGAAGAAAACTATCCA-3'; 5'-TGCTATTCTTCGGCCAGTT-3'. CD44, 5'-AGATCAGTCACAGACCTGC-3'; 5'-AAACTGCAAGAATCAAAGCC-3'. CD24, 5'-TGCTCCTACCCACGCAGATT-3'; 5'-GGCCAACCCAGAGTTGGAA-3'. CD90, 5'-TCAGGAAATGGCTTTTCC-3'; 5'-TCCTCAATGAGATGCCATAAGT-3'. BMI-1, 5'-CCACCTGATGTGTGTGCTTTG-3'; 5'-TTCAGTAGTGGTCTGGTCTTGT-3'. c-MYC, 5'-AATAGAGCTGCTTCGCCTAGA-3'; 5'-GAGGTGGTTCATACTGAGCAAG-3'. onfFN, 5'-ACGTGCCTGGGCAACGGAG-3'; 5'-ACTTCTGGTCGGCATCATA-3'. ALDH1; 5'-CAGACGGGCTGTATGAGTATCT-3'; 5'-ATGGAGGTTGCCAGACGAATC-3'.

Relative mRNA levels were calculated based on the Ct values, corrected for 18S RNA expression, according to the method $2^{-\Delta\Delta Ct}$. All experiments were done in triplicate.

Cell growth assay. To establish growth curves $1x10^5$ cells were cultivated in a 6-cm dish and grown for the indicated times. Cell number was subsequently determined with the CASY1 DT cell counter (Schaerfe Systems). For the determination of mitochondrial activity $1x10^3$ cells were seeded in a 96-well plate and allowed to grow for 7 days. The activity of the mitochondrial dehydrogenases was determined using WST (Roche Diagnostics) according to the manufacturer's instructions. The results for growth kinetics and metabolic activity were derived from three independent cultures.

Transwell migration assay. In vitro chemotaxis was assayed using the HTS Transwell-96 system from Corning (Corning, NY, USA). Cells were serum starved overnight in serum-free medium. 100 μl cells diluted to $75x10^4$/ml in migration buffer (DMEM with 5% BSA) were added in the upper wells, chemoattractants diluted in a serum-free medium were placed to the lower wells. Cells were allowed to migrate for 48 h. Then migrated cells were detached, stained with CyQuant dye and counted using a fluorescence plate reader. All experiments were performed in triplicate.

Flow cytometry sorting. Flow cytometric cell sorting was performed using an Epics Altra flow cytometer (Beckman Coulter, Fullerton, CA, USA). The antibodies used for cell sorting were anti-CD44-FITC and anti-CD24-PE (Pharmingen, Franklin Lakes, NJ, USA). The cells were sorted twice, purity of which was verified by flow cytometry.

Immunohistochemistry. Fixed cells or cryosections (pretreated with 3% hydrogen peroxide in methanol for 5 min to quench endogenous peroxidase activity) were washed in phosphate-buffered saline (PBS) and then blocked for 1 h in washing buffer containing 5% normal goat serum (Sigma). Then the sections were sequentially incubated with mouse antibodies against PCNA and Ki67 antigen (BD Biosciences), biotinylated goat anti-mouse IgG and streptavidin conjugated to horseradish peroxidase. Diaminobenzidine (Dako Corp., Carpinteria, CA, USA) was used for color development. Nuclei were lightly counter stained with hematoxylin. Negative control slides were stained with isotype mouse immunoglobulin in place of primary antibodies.

Western blotting. Total protein was isolated from primary thyroid cancer, primary thyroid cancer-derived tumor stem cell or cells transfected with lenti-let-7a in cell lysis buffer (20 mM Tris, pH 8.0, 100 mM NaCl, 1 mM EDTA, 0.5% Nonidet P-40). Protein concentration was measured using the Bio-Rad protein assay kit. The membrane was first probed with antibodies against Ras (Applied Biomaterials)

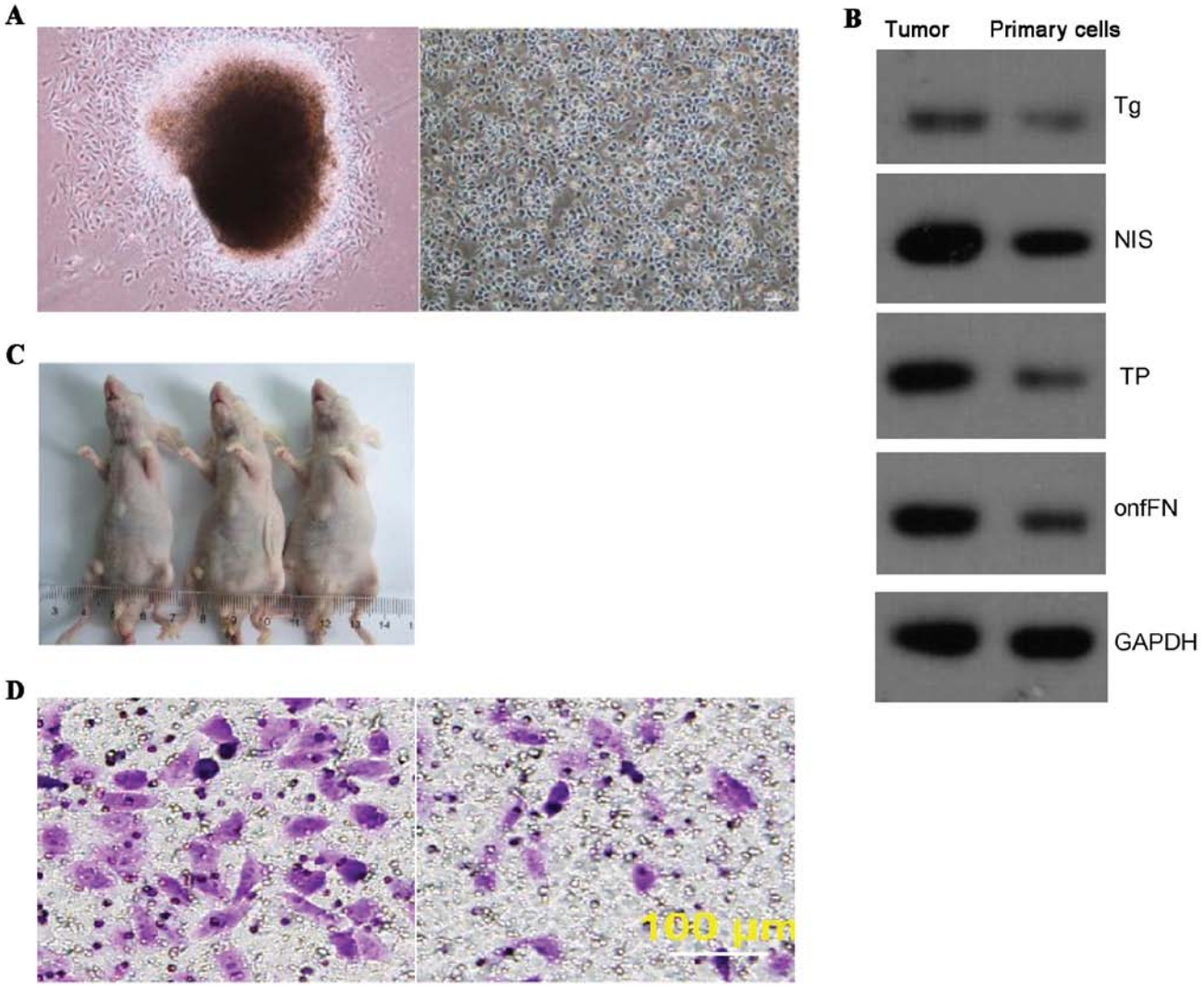

Figure 1. Cultured patient-derived thyroid cancer cells show characteristics of cancer cells. (A) Representative photomicrograph of primary anaplastic thyroid carcinoma cells and the passage 20 in culture. (B) The expression of thyroid cancer specific protein was measured by western blotting. (C) The tumors formed from CSCs were shown in nude mice. (D) Transwell migration assays for cell migration and invasion of p20 ATC cells.

and HMGA2 (Sigma). After being washed extensively three times in TBS-T, samples were incubated in a horseradish peroxidase-conjugated second antibody (1:5,000) at room temperature for an hour, and the blot was developed with ECL reagents (Amersham Biosciences). Western blotting was conducted using standard procedures, using anti-Tg (Sigma), anti-cyclin NIS (Cell Signaling Technology, USA), anti-TP (Cell Signaling Technology), anti-onfFN (Sigma), anti-E-cadherin (Cell Signaling Technology), anti-fibronectin (Sigma), anti-vimentin (Cell Signaling Technology), and anti-INO80 (Sigma). To control for equal sample loading in each group, immunoblotting was performed using antibodies against the cytosolic marker GAPDH (1:5,000, Sigma). The western blotting experiment was repeated at least three times.

Statistical analysis. Data collected from each (experimental and control) group were expressed as the mean ± SEM. One-way analysis of variance and unpaired Student's t-test were performed to analyze the differences between groups using GraphPad Prism 5 program. A P-value <0.01 was denoted as statistically significant between experimental and control groups.

Results

Patient-derived thyroid cancer cells in culture retain characteristics of cancer cells. Primary ATC cells were separated and cultured as described in Materials and methods. Cells from isolated clones were able to maintain original morphology after numerous passages in culture. Tumor formation of $1x10^6$ p20 cells were injected into each nude mouse (Fig. 1A). Western blot analysis revealed notable expression of the thyroid cancer specific proteins such as thyroglobulin (Tg), thyroperoxidase (TPO), sodium/iodide symporter (NIS), and oncofetal fibronectin (onfFN) in passage-20 (p20) cells (Fig. 1B). More importantly, the p20 cells retained the capacity of tumor formation when subcutaneously inoculated in nude mice (Fig. 1C). These cells also showed similar characteristics of invasion (Fig. 1D, left) and migration (Fig. 1D, right) to those observed typically in thyroid cancer cells.

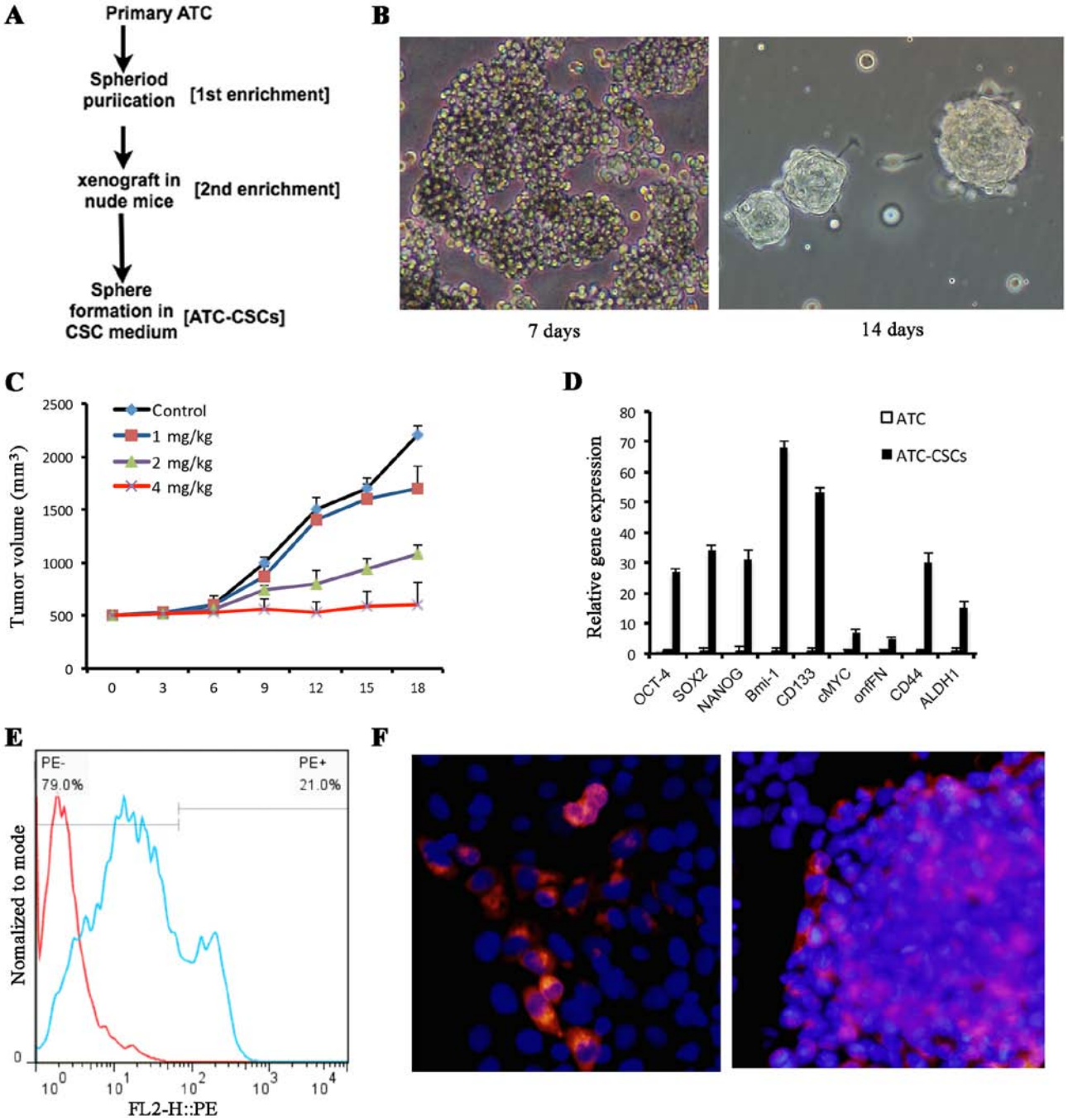

Figure 2. Cisplatin enriches the ATC-CSCs in conditional medium and a xenograft model. (A) The workflow of ATC-CSC purification and enrichment. (B) The morphology of spheres formed by CSCs from p20 cells in suspension culture. (C) Tumor volume in nude mice in response to varying dosage of cisplatin. Data are the mean ± SD of five independent experiments. (D) The mRNA expression of stem cell marker genes in spheres compared with primary cells was detected by qRT-PCR. *P<0.01. (E) The expression of CD133 was detected by flow cytometry. (F) Expression of CD133 was detected by immunofluorescence staining.

Cisplatin treatment enriches ATC-CSCs in a xenograft model. The workflow of ATC-CSC enrichment and isolation is illustrated in Fig. 2A. When grown in a suspension culture system with stem cell specific media and polyhema-precoated dishes, a subpopulation of the p20 cells displayed CSC-like properties as they aggregated and gradually formed spheres after 7-14 days (Fig. 2B). To determine whether this CSC population could be enriched upon chemotherapy, cells collected from the formed spheres were implanted in nude mice to give rise to subcutaneous tumor formation. When the size of tumors reached 5 mm in diameter, the mice were injected intraperitoneally with various doses of cisplatin As shown in Fig. 2C, cisplatin treatment resulted in a dose-dependent tumor inhibition among the xenografts. When given at 4 mg/kg, cisplatin was able to completely abolish the tumor growth over an 18-day period (Fig. 2C). Subsequently, the tumor cells were collected from mice receiving 4 mg/kg cisplatin. The CSC population was expanded based upon the unique capability of its cells to grow and form spheres in the CSC conditional medium. The expression of stem cell marker genes, including OCT-4, SOX2, NANOG, BMI-1, CD133, CD44, C-MYC, onfFN and ALDH1, was found to be consistently upregulated in cells from these

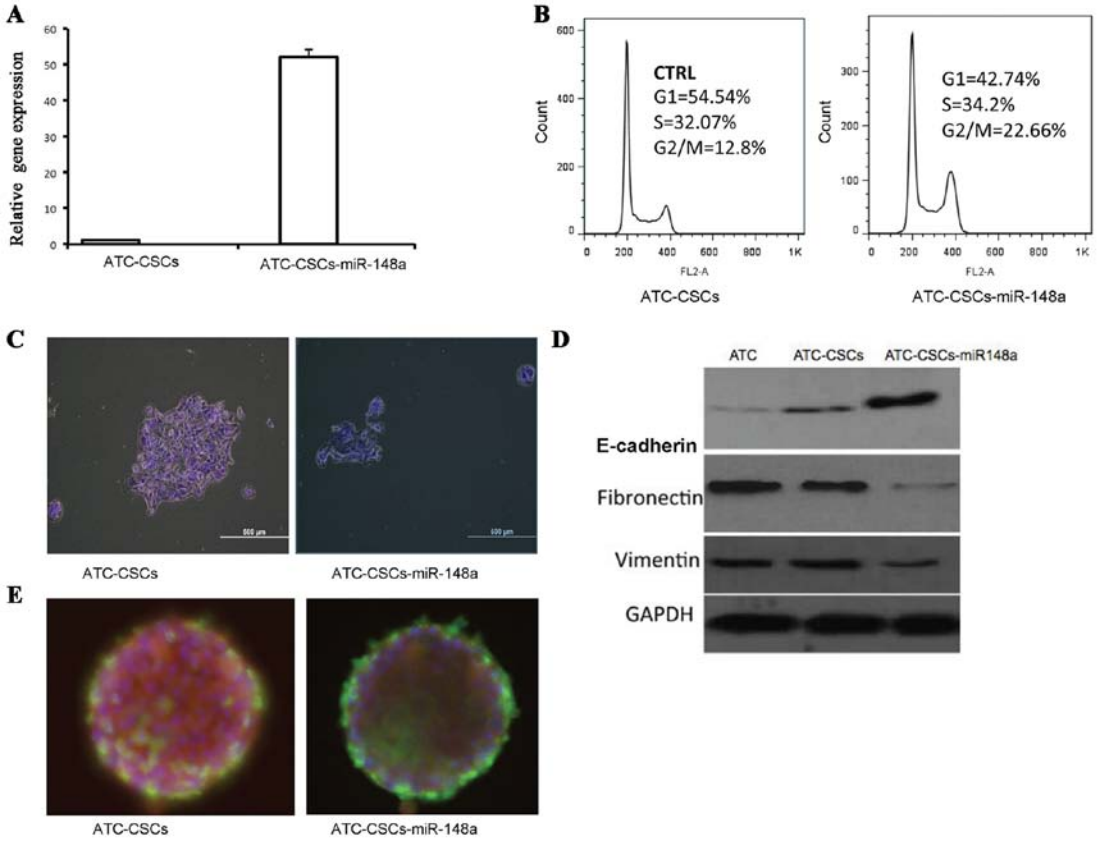

Figure 3. Upregulated miR-148a suppresses stem cell features and EMT of ATC-CSCs. (A) Lentiviral expression of miR-148a was measured by qRT-PCR. *P<0.01, ATC-CSCs vs. miR-148a-overexpressing ATC-CSCs (ATC-CSCs-miR-148a). (B) Cell cycle analysis by PI staining. (C) Cell proliferation after plating in dishes. (D) The protein expression of E-cadherin, fibronectin and vimentin were measured by western blotting. (E) Immunocytochemical staining of OCT-4 and TG in ATC-CSCs and ATC-CSCs-miR-148a.

spheres when compared with the p20 primary cells (Fig. 2D). In addition, both flow cytometry (Fig. 2E) and immunocytochemistry (Fig. 2F) analyses demonstrated that these sphere cells expressed considerably higher levels of the stem cell surface marker CD133. Taking together; these results indicate a potent positive effect of cisplatin in enriching the ATC-CTC population.

Upregulated miR-148a attenuates stem cell features in ATC-CSCs. Next, we performed microarray analysis to identify specific miRNAs whose expression may be differentially regulated in ATC-CSCs vs. primary ATCs. Among 17 miRNAs that showed decreased expression in CSCs, miR-148a exhibited the greatest reduction in ATC-CSCs with a ~150-fold decrease in expression (Table II).

To define the role of miR-148a in ATC-CSCs, we generated a recombinant lentivirus encoding miR-148a. Infection of ATC-CTCs with this virus resulted in a near 50-fold increase in miR-148a expression (Fig. 3A). Interestingly, miR-148a overexpression induced a significant G2/M arrest in ATC-CSCs as revealed by propidium iodide staining (Fig. 3B). Overexpressed miR-148a also significantly inhibited the cell proliferation of ATC-CSCs in adherent culture condition (Fig. 3C). To assess the EMT status of the miR-148a-overexpressing cells, we analyzed expression of the EMT-related proteins including E-cadherin, fibronectin and vimentin. As expected, E-cadherin, an epithelial marker downregulated during EMT,

Table II. Expression of miR-148a is drastically reduced in ATC-CSCs.[a]

Transcript ID (array design)	logFC	FC
hsa-miR-148a	-7.23	-149.60
hsa-miR-192-5p	-5.79	-55.37
hsa-miR-5572	-5.67	-50.80
hsa-miR-3653	-5.66	-50.62
hsa-miR-3613-5p	-5.55	-46.85
hsa-miR-6754-5p	-5.13	-35.13
hsa-miR-185-3p	-4.77	-27.26
hsa-miR-660-3p	-4.76	-27.13
hsa-miR-199b-5p	-4.64	-24.99
hsa-miR-6726-5p	-4.48	-22.30
hsa-miR-1299	-4.47	-22.15
hsa-miR-124-3p	-4.37	-20.68
hsa-miR-7152-3p	-4.35	-20.42
hsa-miR-92a-1-5p	-4.11	-17.22
hsa-miR-1290	-4.02	-16.17
hsa-miR-5093	-3.96	-15.59
hsa-miR-543	-3.95	-15.46

[a]miRNA microarray analysis shows differential expression of specific miRNAs in ATC-CSCs enriched in spheres. The data represent the average of the log2 of the ratios of ATC-CSCs/primary ATCs fluorescence intensity for each specific miRNA.

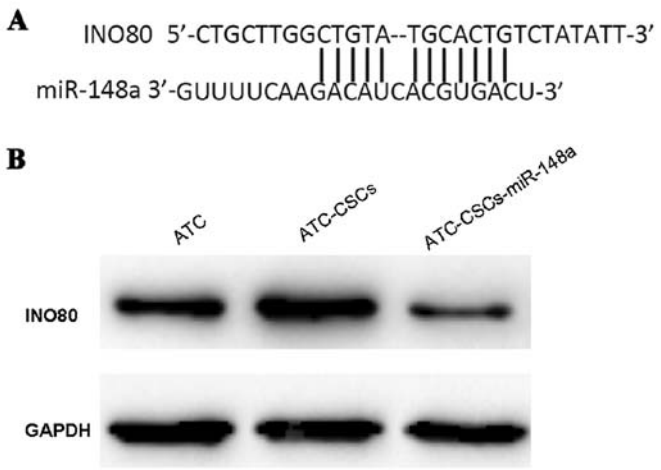

Figure 4. miR-148a targets INO80 and inhibitsits expression in ATC-CSCs. (A) Schematic representation of INO80 and miR-148a-targeted locations. The complementary seed sequence of miR-148a matches a sequence in the 3'UTR of INO80. (B) The protein expression of INO80 was measured by western blotting ATC-CSCs vs. miR-148a-overexpressing ATC-CSCs (ATC-CSCs-miR-148a). ***P<0.01.

was expressed at higher levels in ATC-CSCs than in ATCs. Overexpression of miR148a further increased E-cadherin in ATC-CSCs (Fig. 3D). On the other hand, expression of fibronectin and vimentin, two EMT-associated makers, was significantly suppressed in miR-148a-overexpressing CSCs (Fig. 3D). Moreover, immunofluorescence analysis revealed a decreased staining for stem cell marker OCT-4 in miR148-overexpressing cells along with an increased staining for TG, a marker for differentiated cells (Fig. 3E). Collectively, these results suggest that miR148a may act to impede stemness in ATC-CSCs via downregulating EMT.

miR-148a targets INO80 in ATC-CSCs. To understand the mechanisms underlying the role of miR-148a, we searched for predicted targets of miR-148a using the Target Scan software. INO80, a chromatin remodeler important for endothelial stem cell (ESC) self-renewal, was subsequently identified as a potential target with high confidence score. Sequence analysis further showed that miR-148a could directly target the 3'UTR region of INO80 transcript (Fig. 4A). Overexpression of miR-148a was sufficient to induce a significant reduction of INO80

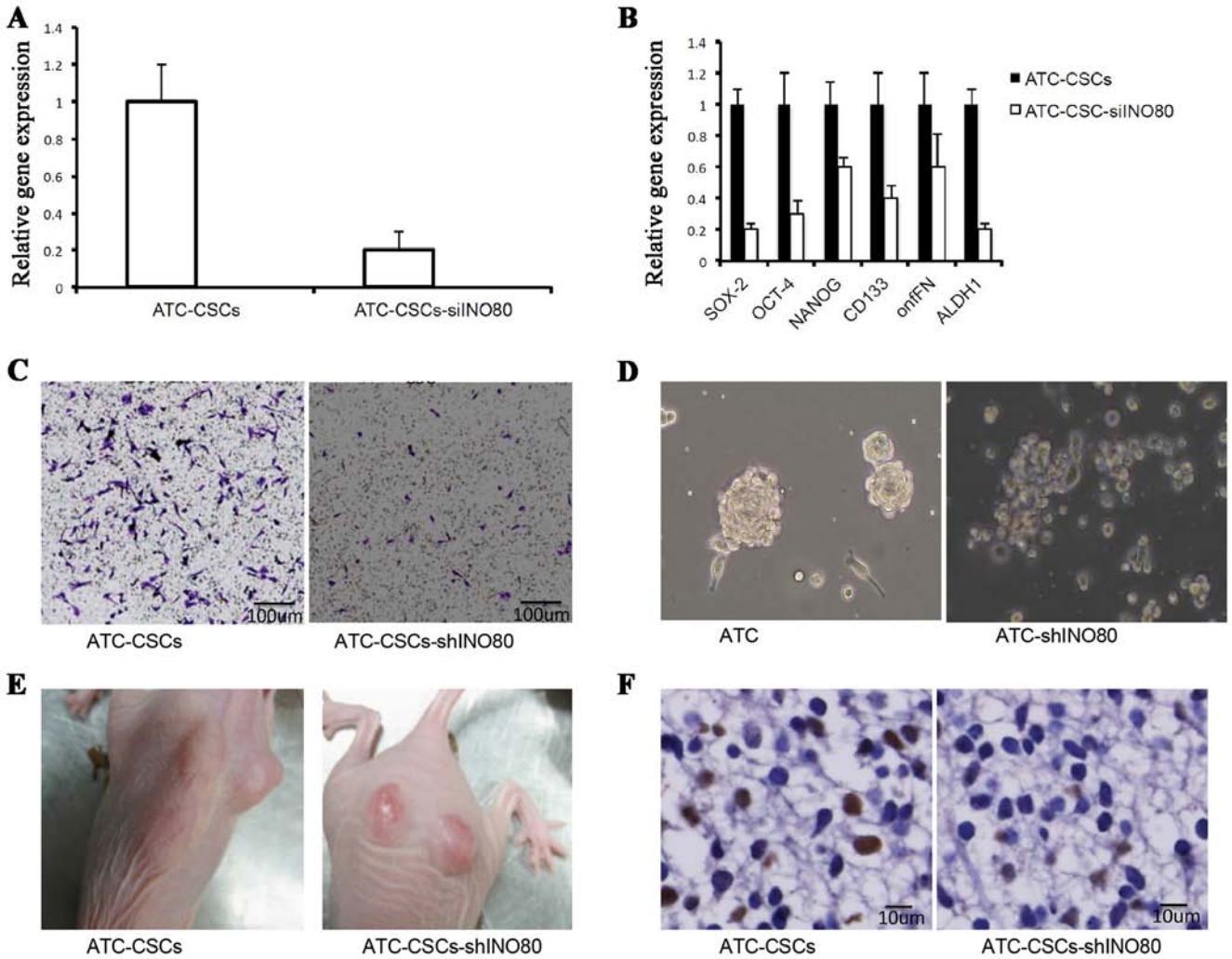

Figure 5. The INO80 is required for stem cell gene expression and tumor forming capability of CSCs. (A) The expression of INO80 was measured by qRT-PCR. *P<0.01, ATC-CSCs and vs. ATC-CSCs infected with lentivirus encoding shINO80 (ATC-CSCs-shINO80). (B) The mRNA expression of stem cell marker genes was detected by qRT-PCR. *P<0.01. (C) Cell migration assay. (D) Sphere formation by ATC-CSCs and ATC-CSCs-shINO80. (E) The xenograft tumors formed by ATC-CSCs and ATC-CSCs-shINO80. (F) Immunocytochemical staining with PCNA.

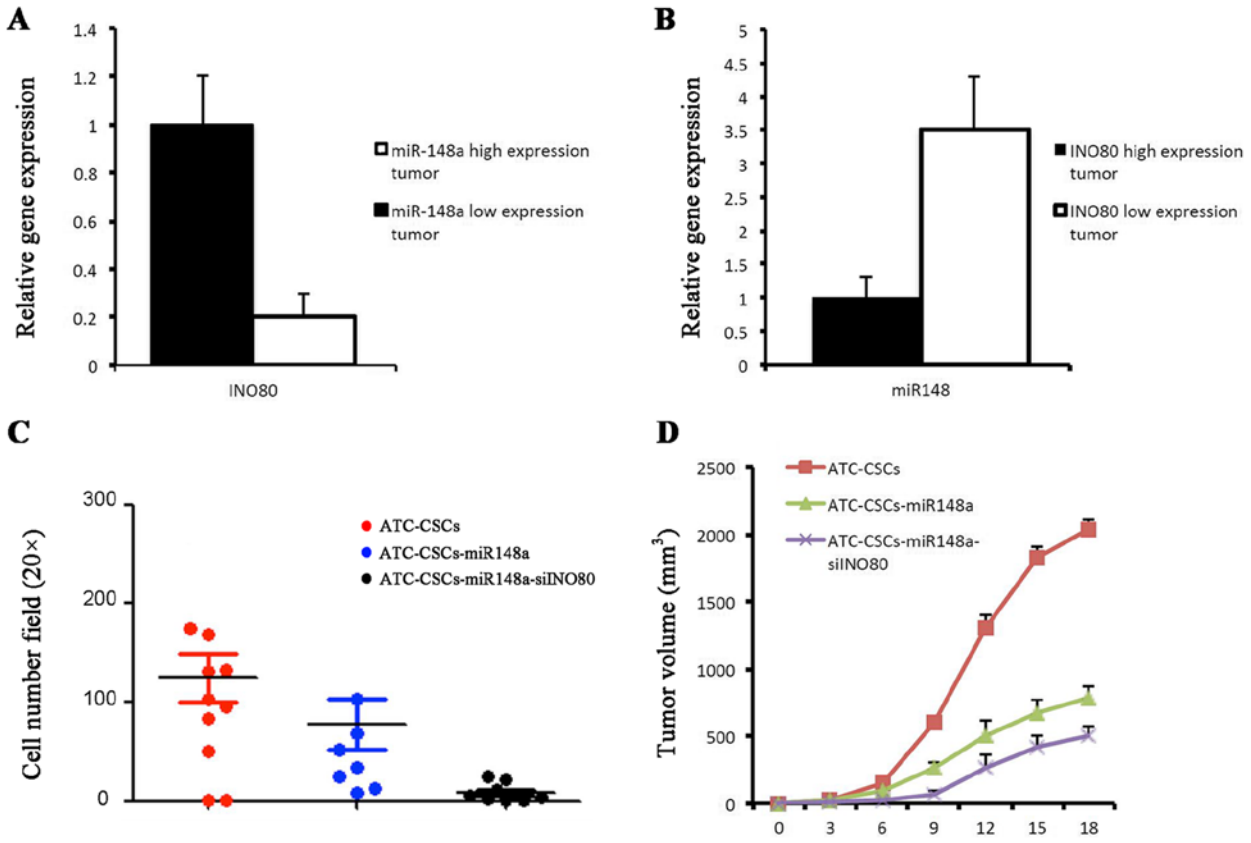

Figure 6. Contrasting roles of miR-148a and INO80 in tumor formation *in vivo*. (A) The expression of INO80 was measured in tumors with different miR-148a levels by qRT-PCR. *P<0.01. (B) The expression of miR-148a was measured in tumors with different INO80 expression by qRT-PCR. *P<0.01. (C) The migration of ATC-CSC stable clones was measured by Tanswell assays. *P<0.01. (D) Volume of xenograft tumors formed by cells from different ATC-CSC stable clones. *P<0.01.

expression in ATC-CSCs (Fig. 4B), confirming the direct regulation of INO80 by miR-148a in living cells.

INO80 is required for CSC gene expression and tumor formation. To determine whether INO80 regulates self-renewal of CSCs and the expression of stem cell-specific genes, we performed knockdown experiments using a lentivirus encoding a shRNA specifically targeting INO80 (shINO80). The tumor formation of $5x10^5$ of ATC-CSCs cells, ATC-CSCs-shINO80 were injected into nude mice, respectively, and were measured 2 weeks later. As shown in Fig. 5A, infection with such virus significantly suppressed INO80 expression in CSCs. Importantly, INO80 knockdown led to the downregulation of various stem cell-specific factors, including OCT-4, SOX2, NANOG, CD133, onfFN and ALDH1 (Fig. 5B), suggesting that INO80 positively regulates the stem cell characteristics. Transwell assays demonstrated that the migration of ATC-CSCs was also inhibited when transduced with the shINO80 virus (Fig. 5C).

To evaluate the effect of shINO80 on sphere-forming potentials, we cultured cells infected with or without shINO80 virus in a non-adhesive culture system. As shown in Fig. 5D, the cells unexposed to shINO80 virus were able to form spheres, whereas those infected with shINO80 virus (ATC-CSCs-shINO80) failed to do the same. Upon inoculation into nude mice, ATC-CSCs-shINO80 form tumors that were significantly smaller in size than those originated from control ATC-CSCs (Fig. 5E). Additionally, a significantly reduced staining for cell proliferation marker PCNA was observed in tumors from ATC-CSCs-shINO80 (Fig. 5F). Overall, these results suggest that the ability of ATC-CSCs to form spheres *in vitro* and tumors *in vivo* are both repressed upon INO80 knockdown.

Roles of miR-148a and INO80 in tumor formation in vivo. Using qPCR assay, we found an inverse relationship between the expression of miR-148 and INO80 in primary ATC samples. Tumors in which miR-148a was downregulated exhibited increased expression of INO80, and vice versa (Fig. 6A and B). To explore miR-148a and INO80 as potential therapeutic targets in the treatment of ATC, we established ATC-CSC clones stably expressing either miR-148a alone or miR-148a with shINO80. In Tanswell assays miR-148a and shINO80 showed synergistic effects in inhibiting cell migration (Fig. 6C). In the nude mouse xenograft model, ATC-CSCs overexpressing miR-148a alone gave rise to tumors that were markedly smaller than those derived from control ATC-CSCs. Coexpression of shINO80 with miR-148a was able to further reduce the tumor volume (Fig. 6D). Taken together, these results suggest a possibility of preventing CSC-initiated tumor formation through combining approaches that upregulate miR-148a and downregulate INO80.

Discussion

In this study, we have successfully purified and enriched a CSC population from primary ATC samples. The derived ATC-CSCs were capable of forming spheres in culture and tumors *in vivo* with high expression of stem cell markers. In our data, thyroid cancer specific proteins Tg, TPO, NIS, and onfFN were expressed in passage-20 cells. Moreover, we obtained compelling evidence that downregulation of miRNA-148 expression is a key feature of these ATC-CSCs. In line with this notion is the finding that forced expression of miRNA-148a induced cell cycle arrest, inhibited proliferation and diminished the overall stemness of ATC-CSCs.

Increasing evidence has pointed to important roles for miR-148a in various forms of tumors such as hepatocellular carcinoma, gastric cancer, pancreatic cancer and colorectal carcinoma (27-30). In particular, miR-148a was recently found to be associated with the growth, invasion and metastasis of tumor cells. To our knowledge, however, this study represents the first to demonstrate that the expression of miR-148a is profoundly lower in ATC-CSCs than in differentiated ATC cells. Although the detailed mechanisms underlying the role of miRNA-148a remain incompletely defined, our data indicate that downregulation of INO80 at least partially accounts for the effects of miRNA-148a overexpression in ATC-CSCs.

The INO80 protein complex was first identified in Saccharomyces cerevisiae for its capability of regulating chromatin structure (31,32). Previous RNAi screens have identified the INO80 complex as a novel self-renewal factor (33,34). INO80 belongs to the INO80 subfamily and is known to participate in a variety of nuclear transactions, including transcriptional regulation, DNA repair and DNA replication (35-37). A recent study provided evidence implicating an essential role of INO80 in the organization of the pluripotency network and the regulation of the pluripotent state (38). This study contributes to the existing knowledge by demonstrating that the expression of INO80 is upregulated in ATC-CSCs, and knockdown of INO80 can significantly decrease the expression of stem cell marker genes.

Several lines of evidence are supportive of INO80 being a direct target of miRNA-148a. Lastly, similar to that observed with miR-148a overexpression, both proliferative and sphere-forming abilities of ATC-CSCs was repressed in response to INO80 knockdown. Data from our functional analysis further demonstrated that the inversed expression of miR-148a and INO80 is critical for ATC-CSCs to maintain their stem cell identity.

In conclusion, in our experiment, we found the expression of INO80 was downregulated upon miRNA-148 overexpression, and knockdown of INO80 can attenuate stem cell-specific properties. We suspect INO80 as a target gene of miR-148a. We will perform additional experiments to prove it. This study offers critical insight into a novel mechanism for the regulation of proliferation and differentiation of thyroid cancer stem cells. Specifically, we provide evidence that miR-148a inhibits the stem cell characteristics of ATC-CSCs via downregulating the expression of INO80. Our findings highlight a potential therapeutic application for targeting INO80 through enhancing miRNA-148a in the treatment of anaplastic thyroid carcinoma. The results that miRNA-148a overexpression along with INO80 knockdown in ATC-CSCs inhibit the volume gain of derived tumors are in strong support of this possibility.

Acknowledgements

This study was supported by Zhongshan Hospital, Fudan University (no. 81070717).

References

1. Shaha AR: Implications of prognostic factors and risk groups in the management of differentiated thyroid cancer. Laryngoscope 114: 393-402, 2004.
2. Kondo T, Ezzat S and Asa SL: Pathogenetic mechanisms in thyroid follicular-cell neoplasia. Nat Rev Cancer 6: 292-306, 2006.
3. Derwahl M: Linking stem cells to thyroid cancer. J Clin Endocrinol Metab 96: 610-613, 2011.
4. Organista-Nava J, Gómez-Gómez Y and Gariglio P: Embryonic stem cell-specific signature in cervical cancer. Tumour Biol 35: 1727-1738, 2014.
5. Kim CF and Dirks PB: Cancer and stem cell biology: How tightly intertwined? Cell Stem Cell 3: 147-150, 2008.
6. Wang Y and Armstrong SA: Cancer: Inappropriate expression of stem cell programs? Cell Stem Cell 2: 297-299, 2008.
7. Gu W, Yeo E, McMillan N and Yu C: Silencing oncogene expression in cervical cancer stem-like cells inhibits their cell growth and self-renewal ability. Cancer Gene Ther 18: 897-905, 2011.
8. Al-Hajj M, Wicha MS, Benito-Hernandez A, Morrison SJ and Clarke MF: Prospective identification of tumorigenic breast cancer cells. Proc Natl Acad Sci USA 100: 3983-3988, 2003.
9. Collins AT, Berry PA, Hyde C, Stower MJ and Maitland NJ: Prospective identification of tumorigenic prostate cancer stem cells. Cancer Res 65: 10946-10951, 2005.
10. Hermann PC, Huber SL, Herrler T, Aicher A, Ellwart JW, Guba M, Bruns CJ and Heeschen C: Distinct populations of cancer stem cells determine tumor growth and metastatic activity in human pancreatic cancer. Cell Stem Cell 1: 313-323, 2007.
11. O'Brien CA, Pollett A, Gallinger S and Dick JE: A human colon cancer cell capable of initiating tumour growth in immunodeficient mice. Nature 445: 106-110, 2007.
12. Schatton T, Murphy GF, Frank NY, Yamaura K, Waaga-Gasser AM, Gasser M, Zhan Q, Jordan S, Duncan LM, Weishaupt C, *et al*: Identification of cells initiating human melanomas. Nature 451: 345-349, 2008.
13. Singh SK, Hawkins C, Clarke ID, Squire JA, Bayani J, Hide T, Henkelman RM, Cusimano MD and Dirks PB: Identification of human brain tumour initiating cells. Nature 432: 396-401, 2004.
14. Friedman S, Lu M, Schultz A, Thomas D and Lin RY: $CD133^+$ anaplastic thyroid cancer cells initiate tumors in immunodeficient mice and are regulated by thyrotropin. PLoS One 4: e5395, 2009.
15. Zito G, Richiusa P, Bommarito A, Carissimi E, Russo L, Coppola A, Zerilli M, Rodolico V, Criscimanna A, Amato M, *et al*: In vitro identification and characterization of CD133 (pos) cancer stem-like cells in anaplastic thyroid carcinoma cell lines. PLoS One 3: e3544, 2008.
16. Todaro M, Iovino F, Eterno V, Cammareri P, Gambara G, Espina V, Gulotta G, Dieli F, Giordano S, De Maria R, *et al*: Tumorigenic and metastatic activity of human thyroid cancer stem cells. Cancer Res 70: 8874-8885, 2010.
17. Kreso A and Dick JE: Evolution of the cancer stem cell model. Cell Stem Cell 14: 275-291, 2014.
18. Yang ZJ and Wechsler-Reya RJ: Hit 'em where they live: Targeting the cancer stem cell niche. Cancer Cell 11: 3-5, 2007.
19. Wang Q, Liu H, Xiong H, Liu Z, Wang LE, Qian J, Muddasani R, Lu V, Tan D, Ajani JA, *et al*: Polymorphisms at the microRNA binding-site of the stem cell marker gene CD133 modify susceptibility to and survival of gastric cancer. Mol Carcinog 54: 449-458, 2015.
20. Wei XD, He J, Gao JX, Wang JY, Ma BJ and Chen J: Investigation on biological characteristics of $CD133^+$ cancer stem cells in human laryngeal carcinoma Hep-2 cell line. Zhonghua Er Bi Yan Hou Tou Jing Wai Ke Za Zhi 48: 578-583, 2013 (In Chinese).

21. Fan X, Chen X, Deng W, Zhong G, Cai Q and Lin T: Up-regulated microRNA-143 in cancer stem cells differentiation promotes prostate cancer cells metastasis by modulating FNDC3B expression. BMC Cancer 13: 61, 2013.
22. Bu P, Chen KY, Chen JH, Wang L, Walters J, Shin YJ, Goerger JP, Sun J, Witherspoon M, Rakhilin N, *et al*: A microRNA miR-34a-regulated bimodal switch targets Notch in colon cancer stem cells. Cell Stem Cell 12: 602-615, 2013.
23. Zhang J, Luo N, Luo Y, Peng Z, Zhang T and Li S: microRNA-150 inhibits human CD133-positive liver cancer stem cells through negative regulation of the transcription factor c-Myb. Int J Oncol 40: 747-756, 2012.
24. Cheng Q, Zhang X, Xu X and Lu X: MiR-618 inhibits anaplastic thyroid cancer by repressing XIAP in one ATC cell line. Ann Endocrinol (Paris) 75: 187-193, 2014.
25. Xiong Y, Zhang L and Kebebew E: MiR-20a is upregulated in anaplastic thyroid cancer and targets LIMK1. PLoS One 9: e96103, 2014.
26. Zhang Y, Yang WQ, Zhu H, Qian YY, Zhou L, Ren YJ, Ren XC, Zhang L, Liu XP, Liu CG, *et al*: Regulation of autophagy by miR-30d impacts sensitivity of anaplastic thyroid carcinoma to cisplatin. Biochem Pharmacol 87: 562-570, 2014.
27. Pan L, Huang S, He R, Rong M, Dang Y and Chen G: Decreased expression and clinical significance of miR-148a in hepatocellular carcinoma tissues. Eur J Med Res 19: 68, 2014.
28. Xia J, Guo X, Yan J and Deng K: The role of miR-148a in gastric cancer. J Cancer Res Clin Oncol 140: 1451-1456, 2014.
29. Liffers ST, Munding JB, Vogt M, Kuhlmann JD, Verdoodt B, Nambiar S, Maghnouj A, Mirmohammadsadegh A, Hahn SA and Tannapfel A: MicroRNA-148a is down-regulated in human pancreatic ductal adenocarcinomas and regulates cell survival by targeting CDC25B. Lab Invest 91: 1472-1479, 2011.
30. Zhang H, Li Y, Huang Q, Ren X, Hu H, Sheng H and Lai M: MiR-148a promotes apoptosis by targeting Bcl-2 in colorectal cancer. Cell Death Differ 18: 1702-1710, 2011.
31. Shen X, Mizuguchi G, Hamiche A and Wu C: A chromatin remodelling complex involved in transcription and DNA processing. Nature 406: 541-544, 2000.
32. Papamichos-Chronakis M, Watanabe S, Rando OJ and Peterson CL: Global regulation of H2A.Z localization by the INO80 chromatin-remodeling enzyme is essential for genome integrity. Cell 144: 200-213, 2011.
33. Chia NY, Chan YS, Feng B, Lu X, Orlov YL, Moreau D, Kumar P, Yang L, Jiang J, Lau MS, *et al*: A genome-wide RNAi screen reveals determinants of human embryonic stem cell identity. Nature 468: 316-320, 2010.
34. Hu G, Kim J, Xu Q, Leng Y, Orkin SH and Elledge SJ: A genome-wide RNAi screen identifies a new transcriptional module required for self-renewal. Genes Dev 23: 837-848, 2009.
35. Conaway RC and Conaway JW: The INO80 chromatin remodeling complex in transcription, replication and repair. Trends Biochem Sci 34: 71-77, 2009.
36. Morrison AJ and Shen X: Chromatin remodelling beyond transcription: The INO80 and SWR1 complexes. Nat Rev Mol Cell Biol 10: 373-384, 2009.
37. Watanabe S and Peterson CL: The INO80 family of chromatin-remodeling enzymes: Regulators of histone variant dynamics. Cold Spring Harb Symp Quant Biol 75: 35-42, 2010.
38. Wang L, Du Y, Ward JM, Shimbo T, Lackford B, Zheng X, Miao YL, Zhou B, Han L, Fargo DC, *et al*: INO80 facilitates pluripotency gene activation in embryonic stem cell self-renewal, reprogramming, and blastocyst development. Cell Stem Cell 14: 575-591, 2014.